

# The structural and dynamic properties of 1-bromodecane in urea inclusion compounds investigated by solid-state $^1\text{H}$ , $^{13}\text{C}$ and $^2\text{H}$ NMR spectroscopy

Xiaorong Yang\*<sup>†</sup> and Klaus Müller

For asymmetric guest molecules in urea, the end-groups of two adjacent guest molecules may arrange in three different ways: head–head, head–tail and tail–tail. Solid-state  $^1\text{H}$  and  $^{13}\text{C}$  NMR spectroscopy is used to study the structural properties of 1-bromodecane in urea. It is found that the end groups of the guest molecules are randomly arranged. The dynamic characteristics of 1-bromodecane in urea inclusion compounds are probed by variable-temperature solid-state  $^2\text{H}$  NMR spectroscopy (line shapes, spin–spin relaxation:  $T_2$ , spin-lattice relaxation:  $T_{1Z}$  and  $T_{1Q}$ ) between 120 K and room temperature. The comparison between the simulation and experimental data shows that the dynamic properties of the guest molecules can be described in a quantitative way using a non-degenerate three-site jump process in the low-temperature phase and a degenerate three-site jump in the high-temperature phase, in combination with the small-angle wobbling motion. The kinetic parameters can be derived from the simulation. Copyright © 2011 John Wiley & Sons, Ltd.

**Keywords:** solid-state NMR;  $^1\text{H}$ ;  $^{13}\text{C}$  and  $^2\text{H}$ ; structure and dynamics; 1-bromodecane; urea inclusion compounds

## Introduction

Inclusion compounds can be formed by various types of organic or inorganic host compounds. Urea represents a prominent host component. Urea molecules construct linear, parallel one-dimensional channels directed along the *c*-axis of the crystal stabilized via hydrogen bonds. The diameter of these channels is *ca* 5.5–5.8 Å.<sup>[1]</sup> With suitable guest molecules, for instance, *n*-alkane and their derivatives,<sup>[2]</sup> these channels are stable and exhibit a hexagonal structure at room temperature. The structural and dynamic properties of the guest molecules trapped within these channels have been studied extensively.<sup>[3–9]</sup>

Functional groups play an important role for the organization of molecules in supermolecular chemistry. The understanding of functional group interactions and the molecular dynamics can provide useful information for practical applications. Urea inclusion compounds (UICs) are considered as ideal model systems to study the interaction between functional groups of the guest molecules isolated by the urea channels.<sup>[10,11]</sup>

Numerous studies about *n*-alkanes<sup>[3,8,12–25]</sup> and  $\alpha$ ,  $\omega$ -dibromoalkanes<sup>[25–30]</sup> in urea indicate that the guest molecules experience substantial mobility, comprising translational and diffusive motions or jumps about the motional symmetry axis, and the conformation of the end groups is considered to be in almost *all-trans* conformational state.<sup>[9,31–33]</sup>

The previous calorimetric,<sup>[34]</sup> X-ray<sup>[35,36]</sup> studies show that UICs with the guest molecules experience a solid–solid phase. This phase transition is considered to be related to the change of dynamic properties of the guest molecules. In the high temperature, the hexagonal structure of urea channels is stabilized by the fast rotational motion of the guest molecules. In the low-temperature phase, the urea channels are distorted into the

orthorhombic structure which induces the spatial restriction to the guest molecules. Thus, the guest molecules lose the rotational freedom. A dynamic discontinuity happens at the solid–solid phase transition for the UICs with *n*-alkane.<sup>[13]</sup> However, this is not true for UICs with  $\alpha$ ,  $\omega$ -dibromoalkanes, a dynamic discontinuity was postponed to a higher temperature than the phase transition temperature.<sup>[27,37]</sup> In order to get more insight into how the local structure and the dynamic properties of guest molecules in channels are affected by the nature of the guest molecules, in this work the asymmetric guest molecule 1-bromodecane in urea is investigated. Dynamic  $^2\text{H}$  NMR spectroscopy, including variable temperature  $^2\text{H}$  NMR line shape, spin–spin ( $T_2$ ) and spin–lattice ( $T_{1Z}$  and  $T_{1Q}$ ) relaxation studies, is used to explore the dynamic properties of 1-bromodecane, selectively deuterated at the brominated methylene group. The kinetic parameters are derived quantitatively by analyzing the experimental data on the basis of suitable motional models. In addition, the structural order and conformation of the guest molecules are probed by performing  $^1\text{H}$  MAS and  $^{13}\text{C}$  CP/MAS NMR measurements on the non-deuterated guest molecules. The data from  $^{13}\text{C}$   $T_{1\rho}$  and  $^1\text{H}$   $T_{1\rho}$  experiments provide additional information about the motion of the guest molecules.

\* Correspondence to: Xiaorong Yang, Institut für Physikalische Chemie, Universität Stuttgart, Pfaffenwaldring 55, D-70569 Stuttgart, Germany. E-mail: r\_yang2000@yahoo.com

† Present address: Department of Chemistry, Pennsylvania State University, University Park, PA 16802, USA.

Institut für Physikalische Chemie, Universität Stuttgart, Pfaffenwaldring 55, D-70569 Stuttgart, Germany

## Experiment and Data Processing

### Materials

All chemicals were obtained from Aldrich Chemicals and used directly. Selectively deuterated 1-bromodecane-1,1- $d_2$  was prepared as follows:

#### 1-bromodecane-1,1- $d_2$

Ethyl decanoate ( $\text{CH}_3(\text{CH}_2)_8\text{COOC}_2\text{H}_5$ ) was reduced with  $\text{LiAlD}_4$  using standard procedures. The obtained decanol-1,1- $d_2$  was transformed into its bromide by an exchange reaction with  $\text{NaBr}$  in an aqueous solution of sulfuric acid. The product 1-bromodecane-1,1- $d_2$  was purified by distillation.

### Urea inclusion compounds

The UICs were prepared by slowly cooling warm solutions of 1-bromodecane with urea in methanol. The white needles were filtered, washed with 2,2,4-trimethylpentane and dried.

### Differential scanning calorimetry

Calorimetric studies were accomplished with a differential scanning calorimeter Netzsch DSC 204 (Selb/Germany) under nitrogen flow at heating rates of  $10^\circ\text{C}/\text{min}$ .

### NMR studies

$^{13}\text{C}$  CP/MAS,  $^1\text{H}$  MAS and  $^2\text{H}$  NMR experiments were performed on a Bruker CXP 300 (Rheinstetten/Germany) spectrometer operating at a static magnetic field of 7.04 T interfaced to a Tecmag spectrometer control system. The resonance frequencies were 75.47 MHz ( $^{13}\text{C}$ ), 300.13 MHz ( $^1\text{H}$ ) and 46.07 MHz ( $^2\text{H}$ ). A double tuned Bruker 4-mm MAS probe was used for the  $^{13}\text{C}$  CP/MAS,  $T_{1\rho}$  ( $^{13}\text{C}$ ) and  $T_{1\rho}$  ( $^1\text{H}$ ) experiments.  $\pi/2$  pulse lengths were 4  $\mu\text{s}$ . Contact times were 1.5 ms, and recycle delays of 6 s were set between successive scans. A sample rotation frequency of 5 kHz was used, and the number of scans was between 512 and 1024. Standard spin-lock pulse sequences were used for the determination of  $^{13}\text{C}$  and  $^1\text{H}$   $T_{1\rho}$  relaxation times.<sup>[38,39]</sup>  $^1\text{H}$  MAS spectra were measured with a Bruker CXP 2.5 mm double resonance MAS probe with a  $\pi/2$  pulse length of 4  $\mu\text{s}$  at a sample rotation frequency of 34 kHz. Typically, 32 scans were accumulated with recycle delays of 2 s.  $^{13}\text{C}$  chemical shifts were referenced to the external standard adamantane. This value was then expressed relative to TMS ( $\delta = 0$  ppm). Likewise,  $^1\text{H}$  chemical shift values were given relative to TMS.

The quadrupole echo sequence  $(\pi/2)_x - \tau_e - (\pi/2)_y - \tau_e$  with a  $\pi/2$  pulse of 2.0  $\mu\text{s}$  and a pulse spacing of  $\tau_e = 20$   $\mu\text{s}$  was used to obtain the experimental  $^2\text{H}$  NMR spectra. Spin–spin relaxation times ( $T_2$ ) were determined with the same pulse sequence by the variation of  $\tau_e$ . A modified inversion recovery sequence,  $\pi - \tau_r - (\pi/2)_x - \Delta - (\pi/2)_y - \Delta$ , combined with the quadrupolar echo sequence for signal detection and variable relaxation intervals  $\tau_r$ , was employed for the determination of  $T_{1Z}$  (relaxation time for Zeeman order). Here, instead of the inversion  $\pi$  pulse, a composite pulse, given by  $[\pi/2]_\phi[\pi/2]_{\phi\pm\pi/2}[\pi/2]_\phi$  with appropriate phase cycling ( $\phi = 0, \pi/2, \pi$  and  $3\pi/2$ ) was used.<sup>[40]</sup> Recycle delays were set to be at least five times the spin–lattice relaxation time  $T_{1Z}$ . Relaxation times for quadrupolar order,  $T_{1Q}$ , were measured by the broadband Jeener–Broekaert sequence (BBJB)

$(90_x^\circ - 2\tau_w - 67.5_y^\circ - 2\tau_w - 45_y^\circ - \tau_w - 45_y^\circ - \tau_r - 45_x^\circ - \Delta - 90_x^\circ)$ .<sup>[41]</sup> Here,  $(90_x^\circ - 2\tau_w - 67.5_y^\circ - 2\tau_w - 45_y^\circ - \tau_w - 45_y^\circ)$  represents the excitation sequence, whose phase cycle maximizes quadrupolar order while fully suppressing Zeeman order.<sup>[42]</sup> A refocusing pulse was used to generate an echo, resulting in partially relaxed spectra with minimal baseline distortion and no first-order phase corrections. The number of scans varied between 512 and 1200 depending on the signal/noise ratio. For the variable temperature experiments, the temperature was controlled by a Bruker BVT 2000 temperature control unit. The samples were initially held at each new temperature for at least 15 min to allow equilibration. The sample temperature was found to be stable within  $\pm 1$  K.

### Data processing and simulations

Data processing of the experimental (from the CXP 300 NMR spectrometer) and theoretical  $^2\text{H}$  NMR signals were done on a SUN workstation by using NMR1 and Sybyl/Triad software packages (Tripos, St. Louis, MO, USA). The data from  $^1\text{H}$  MAS and  $^{13}\text{C}$  CP/MAS NMR measurements were handled by utilizing the MestRec software.<sup>[43]</sup>

The programs employed during the simulations of the corresponding line shape and relaxation experiments are very general, and consider various types of molecular motions of the systems under investigation.<sup>[13,37]</sup> The theoretical line shapes and relaxation times were obtained by numerical diagonalization of the corresponding relaxation matrices by using standard software packages.<sup>[37,44]</sup>

For the line shape simulations, a slow-motional approach was used.<sup>[44,45]</sup> This approach assumes  $\delta$ -pulses and explicitly accounts for the interval  $\tau_e$  in the quadrupolar echo experiment, responsible for spin–spin relaxation. The theoretical description of the spin–lattice relaxation data ( $T_{1Z}$ ,  $T_{1Q}$ ) is based on the Redfield approach.<sup>[46]</sup> Here, partially relaxed spectra were obtained after multiplication of motionally averaged  $^2\text{H}$  NMR spectra (fast exchange limit) with theoretical damping factors that account for orientation-dependent spin–lattice relaxation during the interval  $\tau_r$  of the inversion recovery<sup>[45]</sup> and BBJB experiments.<sup>[41]</sup>

## Results and Discussions

Variable temperature  $^2\text{H}$  NMR spectroscopy was carried out between 120 K and room temperature on UICs with 1-bromodecane selectively deuterated at the end  $\text{CH}_2\text{Br}$  group (Fig. 1). Solid-state  $^1\text{H}$  MAS and  $^{13}\text{C}$  CP MAS NMR studies were performed for the inclusion systems of non-deuterated guest species. Differential scanning calorimetry shows that the phase transition arising from the distortion of the urea channel for 1-bromodecane/urea occurs at ca 133 K. This phase transition temperature is lower than that of 1,10-dibromodecane/urea (141 K)<sup>[26,27,35]</sup> but higher than the value of *n*-decane/UICs which has a phase transition temperature of 111 K.<sup>[34,35]</sup> shown in Table 4. Obviously, the solid–solid phase transition is shifted to higher temperature with the increase of Br substituent number. This implies that the change in urea crystal symmetry from the orthorhombic to the hexagonal form, established by X-ray diffraction,<sup>[34,35,47]</sup> is affected by the Br substituent, most probably due to an increase in intermolecular interactions between the guest and host as well as guest and guest species.

### $^1\text{H}$ MAS and $^{13}\text{C}$ CP/MAS NMR measurements

Figure 2 depicts  $^1\text{H}$  MAS (top trace) and  $^{13}\text{C}$  CP/MAS (bottom trace) NMR spectra of 1-bromodecane/urea. For the  $\text{CH}_3$  group of

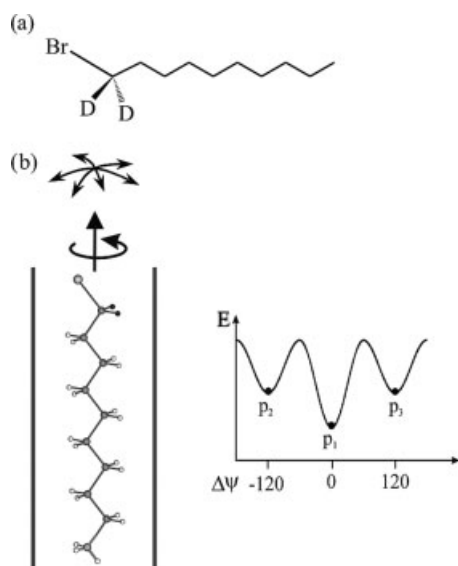


**Figure 1.** (a) Molecular structure for 1-bromodecane-1,1- $d_2$  and (b) possible motions of the guest molecules in urea and schematic drawing of three-site jump motion model.

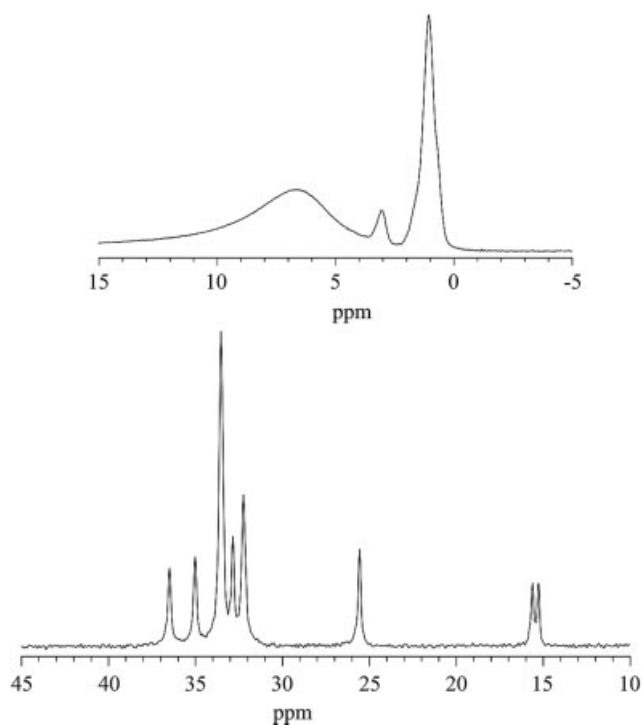


**Figure 2.**  $^1\text{H}$  MAS (top trace) and  $^{13}\text{C}$  CP/MAS (bottom trace) NMR spectra of 1-bromodecane/urea.

1-bromodecane two resonances (15.6 and 15.3 ppm) were observed in the  $^{13}\text{C}$  spectrum, whereas the resonances from other carbons within the molecule appear as single peaks. For asymmetric guest molecules  $\text{X}(\text{CH}_2)_n\text{Y}$  in UICs, the terminal groups of guest molecules can be aligned in three different ways, i.e. head-to-head, tail-to-tail and head-to-tail<sup>[10,11]</sup> two resonances of the terminal groups reflect different terminal group arrangements. A previous report assigned the  $^{13}\text{C}$  resonance of 1-fluorotetradecane/UICs,<sup>[48]</sup> similarly, it is concluded that the

**Table 1.** NMR parameters from  $^{13}\text{C}$  and  $^1\text{H}$  NMR studies on 1-bromodecane in solution and UICs

$\text{C}_{10}\text{H}_{21}\text{Br}$ CT: 1.5 ms	$\delta_{13\text{C}}$ (ppm)		$\delta_{1\text{H}}$ (ppm)		
	Solution <sup>a</sup>	Urea <sup>b</sup>	$\text{C}_{10}\text{H}_{21}\text{Br}$	Solution <sup>c</sup>	Urea <sup>d</sup>
C-1 + Br	33.8	36.5	H-1+Br	3.4	3.5
C-2	33.0	35.0	H-2	1.8	1.5
C-3,4	28.9–28.3	32.2	H-3	1.5	1.5
C-(5–7)	29.5–29.4	33.5	H-(4–9)	1.3	1.5
C-8	32.0	32.9	H-10	0.9	1.1
C-9	22.7	25.6			
C-10··· $\text{CH}_3$	14.1	15.6			
C-10··· $\text{BrH}_2\text{C}$	14.1	15.3			

<sup>a</sup>  $^{13}\text{C}$  chemical shifts of 1-bromodecane in  $\text{CDCl}_3$ .<sup>[58]</sup>

<sup>b</sup>  $^{13}\text{C}$  chemical shifts of 1-bromodecane in their UICs derived in this work from  $^{13}\text{C}$  CP/MAS studies.

<sup>c</sup>  $^1\text{H}$  chemical shifts of 1-bromodecane in  $\text{CDCl}_3$ .

<sup>d</sup>  $^1\text{H}$  chemical shifts of 1-bromodecane in their UICs derived in this work from  $^1\text{H}$  MAS experiments.

resonance at 15.6 ppm reflects  $\text{CH}_3\cdots\text{H}_3\text{C}$  end-group environment while the resonance at 15.3 ppm results from the  $\text{CH}_3\cdots\text{BrH}_2\text{C}$  end-group environment. The intensity ratio of the two resonances is found to be 1 : 1, which indicates that for a given  $\text{CH}_3$  (or  $\text{CH}_2\text{Br}$ ) group, there is an equal chance of having either  $\text{CH}_3$  or  $\text{CH}_2\text{Br}$  as a neighbour – neither alignment is more preferable over the other.

Cross-polarization was used for  $^{13}\text{C}$  NMR spectra recording to improve the signal/noise ratio. In general, the decay of the  $^{13}\text{C}$  signal as a function of contact time is determined by  $^1\text{H} T_{1\rho}$ .<sup>[38,39]</sup> To assess whether the  $\text{CH}_3\cdots\text{H}_3\text{C}$  and  $\text{CH}_3\cdots\text{BrH}_2\text{C}$  peak intensities (the ratio of 1 : 1) relate to the populations of the different sites,  $^{13}\text{C}$  CP MAS NMR spectra are recorded as a function of contact time ranging from 0.5 to 10 ms. The ratio of two resonances (15.6 and 15.3 ppm) remains 1 : 1 for all contact times, which clarifies that the intensities of two end  $\text{CH}_3$  group peaks respond to the population of  $\text{CH}_3\cdots\text{H}_3\text{C}$  and  $\text{CH}_3\cdots\text{BrH}_2\text{C}$  arrangements.<sup>[11,49]</sup>

Likewise, for the  $\text{CH}_2\text{Br}$  end-group, two different environments formed by  $\text{CH}_2\text{Br}\cdots\text{H}_3\text{C}$  and  $\text{CH}_2\text{Br}\cdots\text{BrH}_2\text{C}$  arrangements should co-exist. Thus, it is expected that two resonances corresponding to these two arrangements should be observed. However, only one distinguishable resonance is recorded. This finding indicates that the substituent is the dominant influence on the chemical shift values of the carbon directly bonded to Br atom, compared with  $\text{CH}_2\text{Br}\cdots\text{H}_3\text{C}$  and  $\text{CH}_2\text{Br}\cdots\text{BrH}_2\text{C}$  arrangements. The C–Br bond (1.96 Å<sup>[4]</sup>) is longer than the C–H bond (1.09 Å<sup>[50]</sup>), which results in  $\text{CH}_3$  and  $\text{CH}_2\text{Br}$  end groups not to approach the carbon of the  $\text{CH}_2\text{Br}$  as closely as for the  $\text{CH}_3$  group. And/or the sensitivity of the Br atom feeling the change of the environment is less than the H atom due to Br atom and that this slightly environmental change could not be transmitted to the carbon of  $\text{CH}_2\text{Br}$ . Thus, the carbon nucleus of the end  $\text{CH}_2\text{Br}$  group cannot feel the alternation of the electronic environments resulting from  $\text{CH}_2\text{Br}\cdots\text{H}_3\text{C}$  and  $\text{CH}_2\text{Br}\cdots\text{BrH}_2\text{C}$  arrangements. Therefore, only one resonance (36.5 ppm) for  $\text{CH}_2\text{Br}$  end-group can be resolved.

According to previous studies of UICs containing  $n$ -alkanes with a terminal functional group,<sup>[5,48]</sup> the assignments of  $^1\text{H}$  MAS and  $^{13}\text{C}$  CP/MAS resonances are listed in Table 1 along with the chemical shifts of the corresponding guest molecules in solution. It is found that, in general, the packing effect is responsible for the downfield shift of the  $^{13}\text{C}$  resonances of the guest molecules if

**Table 2.**  $T_{1\rho(13C)}$  and  $T_{1\rho(1H)}$  data for the  $C_{10}H_{21}Br$  in urea

$C_{10}H_{21}Br$ (CT <sup>a</sup> : 1.5 m)	$T_{1\rho(13C)}$ (ms)				$T_{1\rho(1H)}$ (ms) <sup>b</sup>
	294 K	300 K	310 K	320 K	
C-1	196	193	200	268	13
C-2	195	198	232	292	13
C-3,4	190	195	195	258	14
C-(5-7)	182	186	190	232	14
C-8	200	194	225	337	14
C-9	252	254	257	322	13
C-10 ···CH <sub>3</sub>	249	279	262	425	8.8
C-10 ···BrH <sub>2</sub> C	298	227	209	298	9.0

<sup>a</sup> Contact time.<sup>b</sup> Value at 294 K.

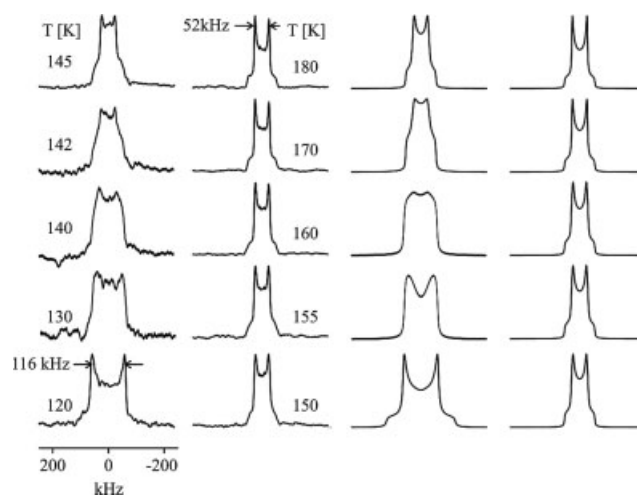
compared with the signals in solution.<sup>[5]</sup> Moreover, CH<sub>2</sub>Br carbon resonance shows a downfield shift of about 2.5 ppm, suggesting that 1-bromodecane in urea adopts an *all-trans* conformation while there is a mutual exchange between the *gauche* and *trans* conformation in solution.<sup>[9,31-33,35,36,51]</sup>

<sup>1</sup>H MAS spectrum of 1-bromodecane in urea exhibits much low resolution, only two resonances are observed, corresponding to the protons of CH<sub>2</sub>Br and the others within the molecules. The nearly same <sup>1</sup>H  $T_{1\rho}$  values are obtained for most of hydrogens in 1-bromodecane. These findings suggest that there is the strong <sup>1</sup>H dipolar coupling in guest molecules. The CH<sub>3</sub> group has a small <sup>1</sup>H  $T_{1\rho}$  value which reflects the end methyl rotation along the chain,<sup>[13,35,52]</sup> as listed in Table 2. Table 2 also gives the temperature-dependent <sup>13</sup>C  $T_{1\rho}$  data. In general, the <sup>13</sup>C  $T_{1\rho}$  data of the carbons within the chain increase with rising temperature, indicating that the motions of guest molecules undergoing are on the high-temperature branch of the relaxation curve. <sup>13</sup>C  $T_{1\rho}$  value decreases towards the center of the chain, which might reflect that overall guest fluctuation motion, being sensitive to the change of the position between the guests and hosts, dominates <sup>13</sup>C relaxation in the rotating frame. It will be shown below that the rotation of the guest molecules along the channel axis is very fast, thus is not expected to affect <sup>13</sup>C  $T_{1\rho}$ .

### Line shapes and spin–spin relaxation times

The temperature-dependent <sup>2</sup>H NMR line shapes, shown in Fig. 3, were recorded between 120 K and room temperature for 1-bromodecane/UICs. The spectrum at 120 K is typical for a static powder pattern, with a 116-kHz splitting between the two perpendicular singularities. Upon sample heating, characteristic variations of the line shapes are observed, indicating that dynamic processes occur with rate constants in the order of the quadrupole coupling constant. Above 160 K, the line shapes are found to be independent of temperature, suggesting that the motion enters the fast exchange limit. Thus, the splitting of the perpendicular singularities remains constant with a value of 52 kHz.

To account for the dynamic properties of the guest molecules, various types of motional models were examined. We tried numerous theoretical simulations which showed that a three-site jump model combined with an overall chain small angle fluctuation can be used to interpret the motion of the guest molecules investigated. Due to the C<sub>6</sub> symmetry of the urea channel, six-site jump model is more realistic for the guest motion.

**Figure 3.** Variable temperature <sup>2</sup>H NMR line shapes of 1-bromodecane-1,1-*d*<sub>2</sub> in urea (left: experiment, right: simulation).

Because three- and six-site models cannot be distinguished, all simulations were done with the three-site jump model. For the three-site jump model (Fig. 1), the angle  $\theta$  between the rotation axis and the C–D bond is set to 90° and the azimuthal angle  $\Delta\phi$  among the jump sites is  $-120^\circ$ ,  $0^\circ$  and  $120^\circ$ , respectively. The sites  $p_2$  and  $p_3$  have identical fractional populations, which are different from the population of the unique site  $p_1$  with a minimum potential, that is  $p_2 = p_3 \neq p_1$ , the summation of the populations of all the three sites is unity ( $p_1 + p_2 + p_3 = 1$ ).

The simulated line shapes are presented in Fig. 3 as well. A best-fit reproduction of the experimental spectrum at 120 K is obtained for the static case with a quadrupole coupling constant of 165 kHz and an asymmetry parameter  $\eta = 0$ . In order to get the good reproduction of the experimental spectra, the quadrupole coupling constant was slightly reduced at elevated temperatures. Above the phase transition, a value of 145 kHz is used. This can be attributed to the occurrence of a fluctuation motion. If the guest molecules undergo a rotational motion in the rapid motional regime (with symmetry  $\geq C_3$ ), the <sup>2</sup>H NMR spectrum regains the axially symmetric Pake powder pattern line shape but its spectral width is half of the spectrum in the slow motional regime.<sup>[13]</sup> However, the experimental results demonstrate that the reduction of the spectral width is more than a factor of 1/2, the additional reduction is attributed to small-angle fluctuations perpendicular to the long molecular axis.

If one motional model is thought to be suitable for a system, it should be possible to reproduce the line shapes as well as the pulse spacing dependence of the line shapes and the spin–spin ( $T_2$ ) relaxation times. The experimental  $T_2$  values (overall powder values) for the 1-bromodecane/urea are plotted in Fig. 4. Figure 5 exhibits two representative series of partially relaxed <sup>2</sup>H NMR spectra, at 130 and 150 K, as a function of the pulse intervals in the quadrupole echo sequence along with the calculated counterparts derived from the assumed three-site jump model. The theoretical partially relaxed <sup>2</sup>H NMR spectra are obtained with the same parameters (population, quadrupole coupling constant and correlation times) as used in the simulations of the <sup>2</sup>H NMR line shapes in Fig. 3. Clearly, the calculated partially relaxed spectra agree very well with the experimental results.

It is also noted that the spectra at 130 K display the properties of two superimposed spectra which may reflect two different

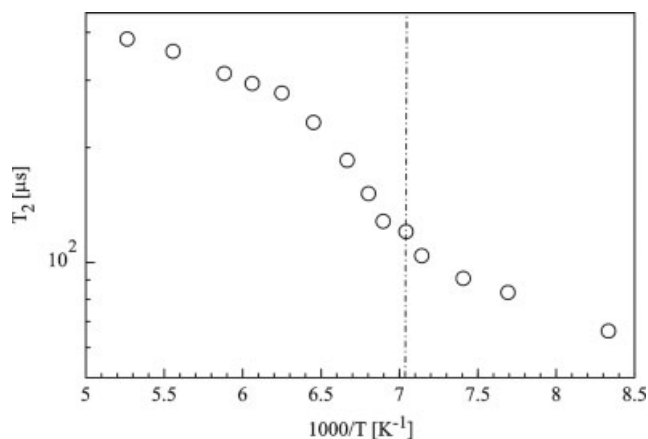


**Figure 4.** Experimental  $^2\text{H}$  spin–spin relaxation data  $T_2$  as a function of temperature for 1-bromodecane-1,1- $d_2$  in urea (dashed line denotes solid–solid phase transition).

end-group arrangements. The inner perpendicular singularities probably relate to the  $\text{CH}_3 \cdots \text{BrCD}_2$  alignment and the outer ones are caused by the large steric hindrance of the  $\text{BrCD}_2 \cdots \text{BrCD}_2$  arrangement. However, the effect of this environmental difference disappears soon with the rising of the temperature as shown by the temperature-dependent lineshapes (Fig. 3).

The simulation of  $^2\text{H}$  NMR line shapes and partially relaxed spectra provides the correlation times for the temperature below 160 K, as listed in Table 3. For a jump model,  $\tau_c$  is related to the jump rate  $k_{ij}$  by

$$\frac{1}{\tau_c} = \frac{k_{ij}}{p_i} \quad (1)$$

where  $p_i$  is the equilibrium population of the site  $i$ . An Arrhenius plot of the correlation times for the three-site jump motion of 1-bromodecane in urea is shown in Fig. 6.

### Spin–lattice relaxation time

If the undergoing motion is in the fast motional limit with correlation times from  $10^{-7}$  to  $10^{-12}$  s, the guest dynamics can

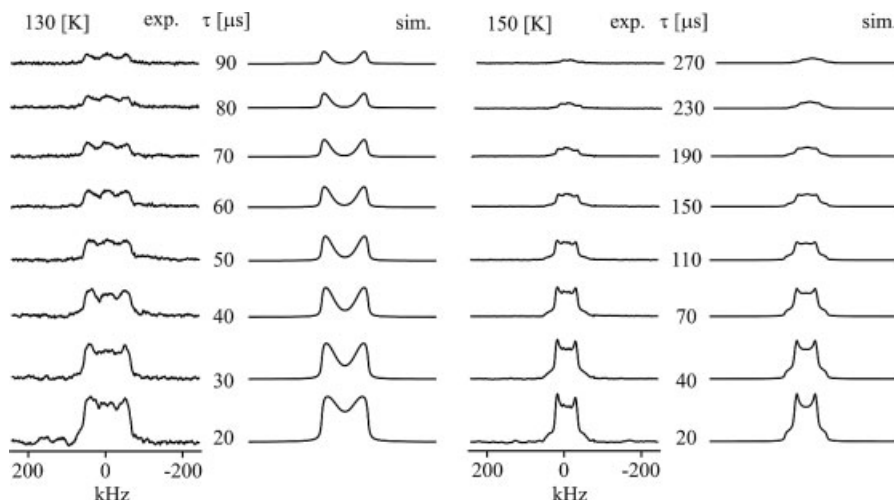


**Figure 5.** Experimental partially relaxed  $^2\text{H}$  NMR spectra from quadrupole echo sequence at 130 and 150 K. The theoretical simulations were done with correlation times  $\tau_c = 6 \times 10^{-7}$  s (130 K) and  $\tau_c = 2 \times 10^{-8}$  s (150 K).

**Table 3.** Simulation parameters for 1-bromodecane-1,1- $d_2$ /urea

Temperature, $T$ (K)	Quadrupole <sup>a</sup> coupl. const., $e^2qQ/h^b$ (kHz)	Correlation time, $\tau_c$ (s)	Population major site, $p_1$	Line width, $1/T_2^0$ ( $\text{s}^{-1}$ )
290	145	$1 \times 10^{-11}$	0.33	1500
280	145	$1.5 \times 10^{-11}$	0.33	1500
270	145	$2 \times 10^{-11}$	0.33	1500
260	145	$2.7 \times 10^{-11}$	0.33	1500
250	145	$3.2 \times 10^{-11}$	0.33	1500
240	145	$4.2 \times 10^{-11}$	0.33	1500
230	145	$6.2 \times 10^{-11}$	0.33	1500
220	145	$8.2 \times 10^{-11}$	0.33	1500
210	145	$1.2 \times 10^{-10}$	0.33	1500
200	145	$1.5 \times 10^{-10}$	0.33	1500
190	145	$1.9 \times 10^{-10}$	0.33	1500
180	145	$2.5 \times 10^{-10}$	0.33	1500
170	145	$3.1 \times 10^{-10}$	0.33	1500
165	145	$3.5 \times 10^{-10}$	0.33	1500
160	145	$1 \times 10^{-8}$	0.36	2000
155	145	$1.8 \times 10^{-8}$	0.36	2500
150	145	$2 \times 10^{-8}$	0.36	2500
145	145	$6 \times 10^{-8}$	0.36	2500
142	145	$2.5 \times 10^{-7}$	0.36	2500
140	145	$4 \times 10^{-7}$	0.36	3000
135	145	$5 \times 10^{-7}$	0.36	3500
130	160	$6 \times 10^{-7}$	0.36	4000
120	165	$1 \times 10^{-4}$	0.36	5000

<sup>a</sup> Quadrupole coupling constant.

<sup>b</sup> Effective values used in the simulations.

be examined in a quantitative way by spin–lattice relaxation experiments.

The experimental and theoretical overall  $T_{1Z}$  data as a function of temperature are given in Fig. 7. A minimum value of 13.7 ms is recorded at 160 K and the two branches separated by the  $T_{1Z}$  minimum value exhibit different slopes. A representative series of partially relaxed  $^2\text{H}$  NMR spectra measured at 170 K from inversion recovery sequence is shown in Fig. 8 together with their theoretical

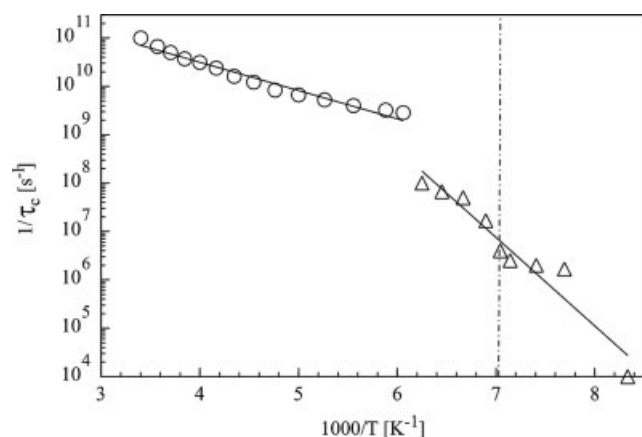


**Figure 6.** Arrhenius plots for the rotational motions of 1-bromodecane-1,1- $d_2$  in urea (dashed line denotes solid–solid phase transition).

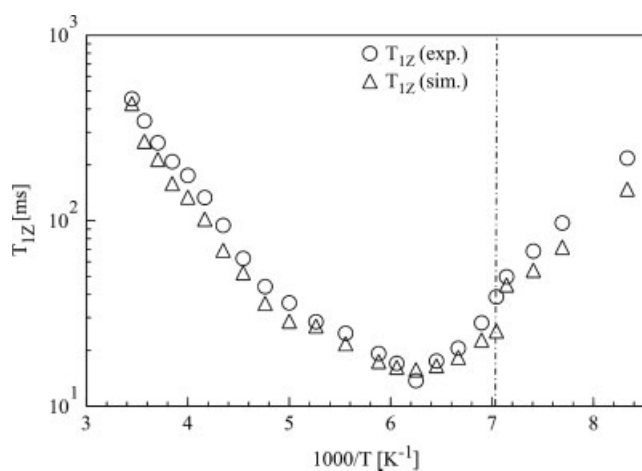


**Figure 7.** Experimental and simulated  $^2\text{H}$  spin–lattice relaxation data  $T_{1Z}$  (Zeeman order) as a function of temperature (dashed line denotes solid–solid phase transition).

counterparts obtained with a jump rate of  $3.2 \times 10^9 \text{ s}^{-1}$ . The good agreement between the experimental and theoretical relaxation data and their anisotropies (visible in the partially relaxed spectra) indicates that the assumed motional model is suitable for the guest dynamics. The obtained correlation times for the temperature above 160 K are listed in Table 3 as well. It is worth mentioning that the theoretical  $T_{1Z}$  data for the temperature below 160 K are calculated with the same parameters used in the simulations of  $^2\text{H}$  NMR line shapes and  $T_2$  data.

A further independent proof for the chosen motional model is obtained from the variable temperature  $T_{1Q}$  data and partially relaxed  $^2\text{H}$  NMR spectra (Figs 9 and 10). Again, the theoretical spectra and  $T_{1Q}$  values were derived by using the same simulation parameters as taken in  $T_{1Z}$  data analysis. The good reproduction of these later experimental data further supports the used three-site jump model for the present system.

It should be emphasized again that for the simulations of the experimental data (including line shapes,  $T_2$ ,  $T_{1Z}$  and  $T_{1Q}$ ) shown above a single set of simulation parameters was used. The population of the major site was slightly changed in order to fit the shape of the perpendicular singularities below 160 K. Here a value of 0.36 was necessary to match the slight inclination of

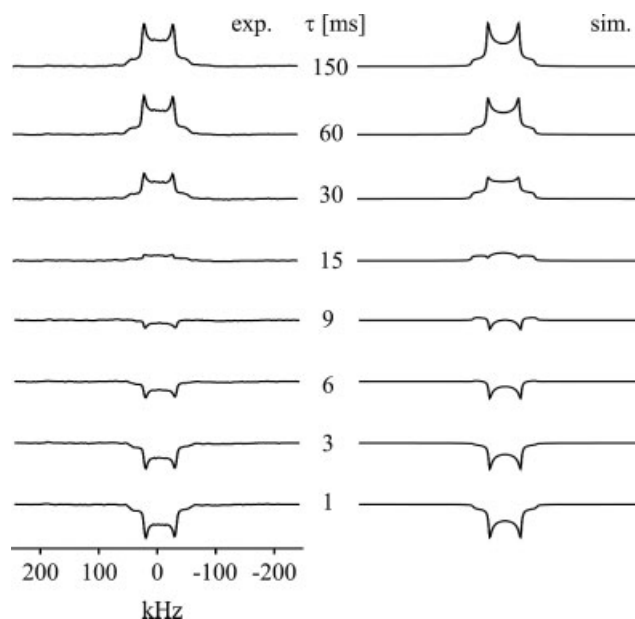


**Figure 8.** Experimental and theoretical partially relaxed  $^2\text{H}$  NMR spectra from inversion recovery experiments at 170 K (correlation time  $\tau_c = 3.1 \times 10^{-10} \text{ s}$ ).

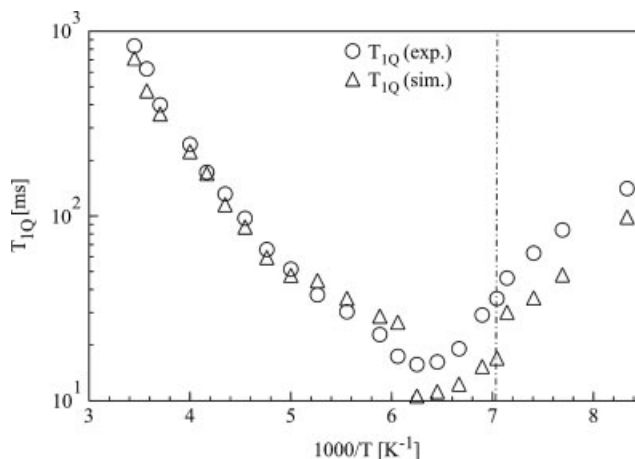


**Figure 9.** Experimental and simulated  $^2\text{H}$  spin–lattice relaxation data  $T_{1Q}$  (quadrupolar order) as a function of temperature (dashed line denotes solid–solid phase transition).

the perpendicular singularities, while above 160 K a value of 0.33 has been taken. The line width ( $1/T_2^0$ ) was varied from 5 kHz at 120 K to 2 kHz at 160 K, which can be attributed to a loss of the heteronuclear dipolar interactions between the guest molecules and the rigid urea matrix due to the increased mobility at higher temperature. Similar observations were reported previously.<sup>[13,27]</sup>

From the Arrhenius plot of the correlation times (Fig. 6), for the high-temperature phase an activation energy of  $11 \pm 0.6 \text{ kJ/mol}$  was determined, whereas  $35 \pm 4 \text{ kJ/mol}$  is derived for the low-temperature phase, which correspond to the two different slopes of the high- and low-temperature phases separated by  $T_{1Z}$  and  $T_{1Q}$  minima at the  $T_{1Z}$  and  $T_{1Q}$  curves, respectively. When reproducing the experimental  $T_{1Z}$  and  $T_{1Q}$  values, it is found that the theoretical  $T_{1Z}$  and  $T_{1Q}$  minima (5.5 and 5.5 ms) do not match with the experimental ones (13.7 and 13.7 ms). That is, the values of the

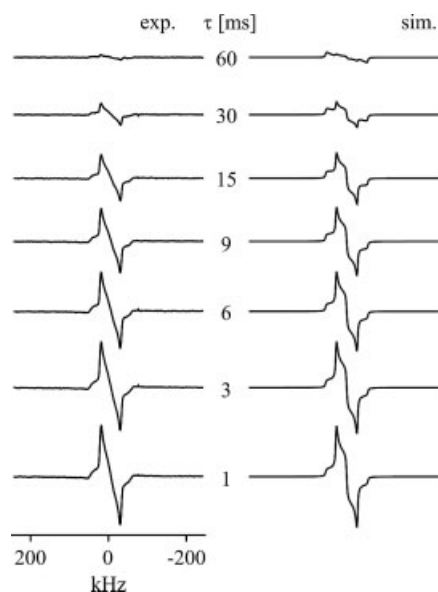


**Figure 10.** Experimental and theoretical partially relaxed  $^2\text{H}$  NMR spectra from broadband Jeener–Broekaert experiments at 170 K (correlation time  $\tau_c = 3.1 \times 10^{-10}$  s).

theoretical  $T_{1Z}$  and  $T_{1Q}$  minima were somehow lower than those for the experimental  $T_{1Z}$  and  $T_{1Q}$  minima. The only way to reproduce the experimental data was by shifting the correlation times to smaller values; therefore, a discontinuity of the correlation time in Arrhenius plot is observed at the temperature corresponding to the  $T_{1Z}$  and  $T_{1Q}$  minima. This phenomenon was also reported for other systems.<sup>[27,53]</sup> Attempts were made to overcome this discontinuity, for instance, by reducing the quadrupole coupling constant, varying the site population and using the distribution of the correlation time. However, none of these attempts were successful. Therefore, these options were not taken into account any further.

The discontinuity of the correlation time is therefore ascribed to the change of urea lattice structure and the type of the guest molecules. For *n*-alkane/UICs, this discontinuity takes place at phase transition temperature<sup>[13]</sup> where the average symmetry of urea channel structure changes from orthorhombic in low-temperature phase to hexagonal in high-temperature phase.<sup>[35,52]</sup> Pronounced changes in the  $T_1$  and  $T_2$  data and  $^2\text{H}$  NMR spectra were observed for this system at the phase transition, which were associated with the abrupt change in the dynamic properties of the guest molecules.<sup>[13]</sup> Above the phase transition temperature the symmetry of the urea channels allows the alkyl chains to rotate rapidly and almost unrestrictedly around the channel long axis, while below the phase transition the alkyl chains were found to experience fast but restricted rotational motions due to the loss of the symmetry of the urea channels.<sup>[13]</sup> However, for di- or mono-bromoalkane/UICs, the bromine atom has a larger diameter compared with that of a proton and/or the C–Br bond is longer relative to the C–H bond. When di- or mono-bromodecane is included within the confined space of the urea channel, the long C–Br bond and/or the large diameter of Br atom can protrude the guest molecules to move toward the channel wall, which induces a repulsive local interaction and results in some local distortion of the host structure. Thus, the urea channel imposes more resistance to the motion of guest molecules. Even across the phase transition temperature, with a slightly enlarged

diameter of the urea channel, the dynamic properties of the guest molecules cannot alter dramatically. No discontinuity at the phase transition temperature can be observed in the  $T_1$  and  $T_2$  curves for di- or mono-bromoalkane/UICs<sup>[26,27]</sup>; in contrast, a pronounced discontinuity occurs for *n*-alkane/UICs.<sup>[13]</sup> It is thus found that the dynamic properties of the guest molecules continuously change with the elevating temperature even crossing the phase transition temperature. Once the effect of local distortion of the urea channels caused by the long C–Br bond (1.96 Å<sup>[4]</sup>) and/or the large diameter of the Br atom is eliminated by a widening of the channel diameter, the motion of the guest molecules becomes suddenly very fast. A similar discontinuity of the dynamic properties of the guest molecules at the temperature corresponding to the  $T_{1Z}$  minimum, as reflected by a discontinuity of the Arrhenius plots, is also observed for di- or mono-bromoalkane/UICs.<sup>[27,37]</sup>

The phenomenon that the transition of the molecular behaviour of the guests is delayed to a higher temperature than the phase transition temperature was also observed in stearic acid/UICs.<sup>[54]</sup> Raman spectroscopy showed that there were abrupt discontinuities in the behaviour of the bands from urea at the temperature range of 232–236 K (only within an interval of 4 K), as a consequence of the phase transition centered at  $\sim 234$  K. In contrast, the Raman bands of the guest molecule stearic acid displayed a continuous change in the range from 223 to 253 K, i.e. a transition covering  $\sim 30$  K. Thus, it can be concluded that the molecular behaviour of the guests in urea is related to both the change of the urea lattice matrix and the type of the guest molecules, and that the structural changes of the urea host lattice do not necessarily correlate with discontinuous changes of the guest motions.

It is found from the  $T_{1Q}$  curve in Fig. 9 that the theoretical  $T_{1Q}$  values slightly deviate from the experimental counterparts in the low-temperature phase. A possible explanation is  $T_{1Q}$ , which only depends on  $J_1(\omega_0)$ , is far more sensitive to small angle fluctuations – so far not considered in the  $^2\text{H}$  NMR relaxation data analysis – than  $T_{1Z}$  which additionally contains a contribution from  $J_2(2\omega_0)$ ,<sup>[55,56]</sup> as shown by the expressions

$$\frac{1}{T_{1Z}} = \frac{3\pi^2}{2} (e^2 q_{zz} Q/h)_0^2 (J_1(\omega_0) + 4J_2(2\omega_0)) \quad (2)$$

$$\frac{1}{T_{1Q}} = \frac{9\pi^2}{2} (e^2 q_{zz} Q/h)_0^2 J_1(\omega_0) \quad (3)$$

where  $e^2 q_{zz} Q/h$  is the quadrupole coupling constant,  $J_1$  and  $J_2$  are the spectral density functions. The amplitude of guest fluctuation is extremely sensitive to the channel diameter,<sup>[57]</sup> and this would be larger if the channel is allowed to deform. Therefore, it can be concluded that fluctuations of the guests can affect  $T_{1Q}$  but have negligible effects on the  $T_{1Z}$  data.

For both 1-bromodecane and 1,10-dibromodecane in their UICs,<sup>[27]</sup> the guest dynamics can both be explained in terms of the superposition of a small angle fluctuation and the aforementioned three-site jump model in the temperature range investigated. With respect to the three-site jump model, the comparison of the kinetic parameters for 1-bromodecane/urea and 1,10-dibromodecane/urea shows that at the same temperature, the correlation time is similar. However, the quadrupole coupling constant and the population of the major site are quite different. For instance, for 1-bromodecane an effective quadrupole coupling constant of 145 kHz is found at 135 K, while for 1,10-dibromodecane this value is not observed until 280 K (the small angle fluctuation mainly contributes to the reduction of the

**Table 4.** The structural and dynamic parameters of *n*-decane, 1-bromodecane and 1,10-dibromodecane in urea

Compounds in urea Temperature	P1		PTT (K)	Temp. ( $\tau_c$ jump), K	$\Delta E$ (kJ/mol)		$\Delta H$ (kJ/mol)	Motion model
	120 K	165 K			HTP	LTP	LTP	
<i>n</i> -decane <sup>34,35</sup>			111					
1-Bromodecane	0.36	0.33	133	~163	11	35	72	3-site jump
1,10-Dibromodecane <sup>27</sup>	0.88	0.42	141	~168	13	4.7	~1	3-site jump

PTT, phase transition temperature; P1, population of the site 1;  $\Delta E$ , activation energy;  $\Delta H$ , enthalpy;  $\tau_c$ , correlation time; HTP, high-temperature phase; LTP, low-temperature phase; Temp. ( $\tau_c$  jump), the temperature of the correlation time discontinuity.

spectral width, which is reflected by the reduced quadrupole coupling constant). Likewise, for 1-bromodecane the populations of all three sites are assumed to be equal at 160 K, whereas for 1,10-dibromodecane even at room temperature the population of major site is set as 0.36. For the three-site jump motion in the high-temperature branches of the  $T_{1Z}$  and  $T_{1Q}$  curves, the activation energy of 11 kJ/mol for 1-bromodecane is derived while 13 kJ/mol for 1,10-dibromodecane. These findings indicate that the increasing Br atoms in guest molecules enhance the spatial hindrance of the overall rotation motion. It is also noted that in the low-temperature phase, for 1-bromodecane/urea, it is 35 kJ/mol, while 4.6 kJ/mol for 1,10-dibromodecane. However, the enthalpy of 1,10-dibromodecane calculated from the temperature-dependent population is very large, about 72 kJ/mol although the data points of the population are much scattered and the population of the major is varied from 0.89 to 0.42, while the enthalpy of the 1-bromodecane/urea is very small, about 1 kJ/mol and the population is almost even for three sites, as given in Table 4. Considering these results, it should be reasonably concluded that increasing Br atoms in guest molecules enhances the spatial hindrance of the overall rotation motion even in the low-temperature phase.

For the phase transition temperatures of UICs with *n*-decane, 1-bromodecane and 1,10-dibromodecane it is found that with an increase of Br substituent number in the guest molecules the phase transition temperature is shifted to higher temperatures. The onset of the order–disorder transition of the guest molecules in urea is thus related to the number of the Br atoms because the interaction of the bromine with the channel wall is much stronger than for the proton, and the C–Br bond is longer than the C–H bond as well. The long C–Br bond and/or the large Br atom diameter occupy more space of the urea channel and enhance the steric hindrance for the guest motion. These effects also give rise to the fact that the dynamic discontinuity of the guest motions for di- and mono-bromoalkane/UICs is shifted to a higher temperature than the solid–solid phase transition temperature compared with that for *n*-alkane/UICs. Thus, the guest–host and guest–guest interactions rise with the increase of the Br atom number.

## Conclusions

The structural and dynamic properties of asymmetric guest molecules in UICs are investigated by the multiple-nuclear NMR spectroscopy. <sup>13</sup>C CP MAS NMR studies of 1-bromodecane/UICs reveal that there is no preference for a particular arrangement of the chain ends, i.e. no preference for head–head, head–tail or tail–tail.

The dynamic properties of the 1-bromodecane guests are examined by <sup>2</sup>H NMR spectroscopy including line shape, spin–spin

( $T_2$ ) and spin–lattice relaxation ( $T_{1Z}$  and  $T_{1Q}$  studies). The quantitative analysis of the experimental data shows that a non-degenerate three-site/six-site jump process can be applied to describe the motion of the guests in the low-temperature phase, whereas the dynamic characteristics of the guests in the high-temperature phase are described by a degenerate three-site/six-site jump model. An activation energy of 11 kJ/mol is derived for the high-temperature phase and 35 kJ/mol for the low-temperature phase. For the guest motion a small angle fluctuation, which gives rise to a reduction of the quadrupole coupling constant in <sup>2</sup>H NMR spectra, is also considered in the whole temperature range investigated. It is anticipated that the bromine substituents in guest molecules give rise to stronger guest–host, guest–guest interactions.

## Acknowledgements

The authors thank Mrs. Gabrielle Bräuning for her help during the chemical synthesis and preparation of the samples. Financial support by the Deutsche Forschungsgemeinschaft and the Graduiertenkolleg No. 448 'Modern Methods of Magnetic Resonance in Materials Science' is gratefully acknowledged.

## References

- [1] A. R. George, K. D. M. Harris, *J. Mol. Graphics* **1995**, *13*, 138.
- [2] W. Schlenk, *Liebigs Ann. Chem.* **1949**, *565*, 204.
- [3] T. Nakaoki, H. Nagano, T. Yanagida, *J. Mol. Struct.* **2004**, *699*, 1.
- [4] I. Kanesaka, S. Matsuzawa, T. Ishioka, Y. Kitagawa, K. Ohno, *Spectrochim. Acta A* **2004**, *60*, 2621.
- [5] F. Imashiro, T. Maeda, T. Nakai, A. Saika, T. Terao, *J. Phys. Chem.* **1986**, *90*, 5498.
- [6] R. L. Vold, G. L. Hoatson, R. Subramanian, *J. Chem. Phys.* **1998**, *108*, 7305.
- [7] M. Okazaki, A. Naito, C. A. McDowell, *Chem. Phys. Lett.* **1983**, *100*, 15.
- [8] H. L. Casal, D. G. Cameron, E. C. Kelusky, *J. Chem. Phys.* **1984**, *80*, 1407.
- [9] S. P. Smart, A. E. Baghdadi, F. Guillaume, K. D. M. Harris, *J. Chem. Soc. Faraday Trans.* **1994**, *90*, 1313.
- [10] M. D. Hollingsworth, A. R. Palmer, *J. Am. Chem. Soc.* **1993**, *115*, 5881.
- [11] M. D. Hollingsworth, N. Cyr, *Mol. Cryst. Liq. Cryst.* **1990**, *187*, 135.
- [12] M. S. Greenfield, R. L. Vold, R. R. Vold, *Mol. Phys.* **1989**, *66*, 269.
- [13] J. Schmider, K. Müller, *J. Phys. Chem. A* **1998**, *102*, 1181.
- [14] R. Lefort, B. J. Toudic, J. Etrillard, F. Guillaume, P. Bourges, R. Currat, T. Breczewski, *Eur. Phys. J. B* **2001**, *24*, 51.
- [15] S. Darbha, C. Walee, K. Larry, *J. Phys. Chem.* **1982**, *86*, 4822.
- [16] D. F. R. Gilson, C. A. McDowell, *Mol. Phys.* **1961**, *4*, 125.
- [17] K. Umamoto, S. S. Danyluk, *J. Phys. Chem.* **1967**, *71*, 3757.
- [18] K. D. M. Harris, P. Jonsen, *Chem. Phys. Lett.* **1989**, *154*, 593.
- [19] M. S. Greenfield, R. L. Vold, R. R. Vold, *J. Chem. Phys.* **1985**, *83*, 1440.
- [20] F. Guillaume, C. Sourisseau, A. J. Dianoux, *J. Chem. Phys.* **1990**, *93*, 3536.
- [21] F. Guillaume, C. Sourisseau, A. J. Dianoux, *J. Chim. Phys. (Paris)* **1991**, *88*, 1721.

- [22] B. Toudic, H. Le Lann, F. Guillaume, R. E. Lechner, J. Ollivier, P. Bourges, *Chem. Phys.* **2003**, 292, 191.
- [23] H. Le Lann, B. Toudic, R. Lefont, J. Etrillard, F. Guillaume, B. Ruffle, J. Ollivier, R. E. Lechner, T. Brezczewski, *Physica B* **2000**, 276–278, 298.
- [24] J. Olivier, C. Ecolivet, S. Beaufils, F. Guillaume, T. Brezczewski, *Europhys. Lett.* **1998**, 43, 546.
- [25] J. B. Bell, R. E. Richards, *Trans. Faraday Soc.* **1969**, 65, 2529.
- [26] A. E. Aliev, S. P. Smart, I. J. Shannon, K. D. M. Harris, *J. Chem. Soc. Faraday Trans.* **1996**, 92, 2179.
- [27] X. Yang, K. Müller, *Appl. Magn. Reson.* **2007**, 32, 407.
- [28] F. Guillaume, S. P. Smart, K. D. M. Harris, A. J. Dianoux, *J. Phys. Condens. Mat.* **1994**, 6, 2169.
- [29] S. P. Smart, F. Guillaume, K. D. M. Harris, C. Sourisseau, A. J. Dianoux, *Physica B* **1992**, 180, 687.
- [30] U. Werner-Zwanziger, M. E. Brown, J. D. Chaney, E. J. Still, M. D. Hollingsworth, *Appl. Magn. Reson.* **1999**, 17, 265.
- [31] K. A. Wood, G. G. Snyder, H. L. Strauss, *J. Chem. Phys.* **1989**, 91, 5255.
- [32] H. L. Casal, *J. Phys. Chem.* **1990**, 94, 2232.
- [33] A. El Baghdadi, F. Guillaume, *J. Raman Spectrosc.* **1995**, 26, 155.
- [34] R. C. Pemberton, N. G. Parsonage, *Trans. Faraday Soc.* **1965**, 61, 2112.
- [35] Y. Chatani, H. Anraku, Y. Taki, *Mol. Cryst. Liq. Cryst.* **1978**, 48, 219.
- [36] A. E. Smith, *Acta Crystallogr.* **1952**, 5, 224.
- [37] X. Yang, K. Müller, *J. Mol. Struct.* **2007**, 831, 75.
- [38] E. O. Stejskal, J. Schaefer, M. D. Sefcik, R. A. McKay, *Macromolecules* **1981**, 14, 275.
- [39] J. Schaefer, E. O. Stejskal, R. Buchdahl, *Macromolecules* **1977**, 10, 384.
- [40] N. J. Heaton, R. R. Vold, R. L. Vold, *J. Magn. Reson.* **1988**, 77, 572.
- [41] S. Wimperis, *J. Magn. Reson.* **1990**, 86, 46.
- [42] G. L. Hoatson, *J. Magn. Reson.* **1991**, 94, 152.
- [43] J. C. Cobas, F. J. Sardina, *Concept Magn. Reson. A* **2003**, 19A, 80.
- [44] R. J. Wittebort, E. T. Olejniczak, R. G. Griffin, *J. Chem. Phys.* **1987**, 86, 5411.
- [45] K. Müller, P. Meier, G. Kothe, *Prog. Nucl. Magn. Reson. Spectrosc.* **1985**, 17, 211.
- [46] A. G. Redfield, *Adv. Magn. Reson.* **1965**, 1, 1.
- [47] K. D. M. Harris, S. P. Smart, M. D. Hollingsworth, *J. Chem. Soc. Faraday Trans.* **1991**, 87, 3423.
- [48] A. Nordon, R. K. Harris, L. Yeo, K. D. M. Harris, *Chem. Commun.* **1997**, 21, 2045.
- [49] L. B. Alemany, D. M. Grant, R. J. Pugmire, T. D. Alger, K. W. Zilm, *J. Am. Chem. Soc.* **1983**, 105, 2133.
- [50] R. S. Roy, *J. Phys. B* **1968**, 1, 445.
- [51] R. Forst, H. Jagodzinski, H. Boysen, F. Frey, *Acta Crystallogr.* **1989**, B46, 70.
- [52] K. D. M. Harris, *J. Solid State Chem.* **1993**, 106, 83.
- [53] J. A. Villanueva-Garibay, K. Müller, *J. Phys. Chem. B* **2004**, 108, 15057.
- [54] H. L. Casal, D. G. Cameron, E. C. Kelusky, A. P. Tulloch, *J. Chem. Phys.* **1984**, 81, 4322.
- [55] R. R. Vold, R. L. Vold, *Adv. Magn. Opt. Reson.* **1991**, 16, 85.
- [56] R. L. Vold, R. R. Vold, M. Warner, *J. Chem. Soc. Faraday Trans.* **1988**, 84, 997.
- [57] R. L. Vold, R. R. Vold, N. J. Heaton, *Adv. Magn. Reson.* **1989**, 13, 17.
- [58] J. Elguero, M. Espada, *Anales de Quimica* **1979**, 75, 771.